




FELIX AMBELLAN¹, STEFAN ZACHOW²,
CHRISTOPH VON TYCOWICZ³

An as-invariant-as-possible GL+(3)-based Statistical Shape Model⁴

¹  0000-0001-9415-0859, corresponding author

²  0000-0001-7964-3049

³  0000-0002-1447-4069

⁴to appear in: WKSH on Mathematical Foundations of Computational Anatomy (MFCA)

Zuse Institute Berlin
Takustr. 7
14195 Berlin
Germany

Telephone: +49 30-84185-0
Telefax: +49 30-84185-125

E-mail: bibliothek@zib.de
URL: <http://www.zib.de>

ZIB-Report (Print) ISSN 1438-0064
ZIB-Report (Internet) ISSN 2192-7782

An as-invariant-as-possible $GL^+(3)$ -based Statistical Shape Model

Felix Ambellan^[0000–0001–9415–0859], Stefan Zachow^[0000–0001–7964–3049], and
Christoph von Tycowicz^[0000–0002–1447–4069]

Therapy Planning Group, Zuse Institute Berlin, Berlin, Germany
{ambellan, zachow, vontycowicz}@zib.de

Abstract. We describe a novel nonlinear statistical shape model based on differential coordinates viewed as elements of $GL^+(3)$. We adopt an as-invariant-as possible framework comprising a bi-invariant Lie group mean and a tangent principal component analysis based on a unique $GL^+(3)$ -left-invariant, $O(3)$ -right-invariant metric. Contrary to earlier work that equips the coordinates with a specifically constructed group structure, our method employs the inherent geometric structure of the group-valued data and therefore features an improved statistical power in identifying shape differences. We demonstrate this in experiments on two anatomical datasets including comparison to the standard Euclidean as well as recent state-of-the-art nonlinear approaches to statistical shape modeling.

Keywords: Statistical shape analysis · Tangent principal component analysis · Lie groups · Classification · Manifold valued statistics

1 Introduction

Changes in the shape of anatomies are often early indicators of specific diseases. For example, musculoskeletal disorders affecting large proportions of the adult population such as Osteoarthritis (OA) [17] are associated with morphological changes. The overall socio-economic burden [6] associated with these diseases provides a strong impetus to develop novel computational approaches for the support of treatment and prevention strategies. Statistical models of shape have been established as one of the most successful methods for understanding the geometric variability of anatomical structures [1]. Given a set of samples from an object class under study, statistical shape models estimate the distribution of the underlying population in terms of a mean shape and a hierarchy of principle modes encoding the variation of the samples around that mean. Moreover, representing the samples within the basis of principle modes provides a concise and highly discriminative description that is susceptible for analysis and inference algorithms. In particular, descriptors based on statistical shape modeling have proven effective for predicting the onset and progression of OA [5, 20, 22, 23].

While linear approaches like the *point distribution model* (PDM) [7] are still the most widely used in applied morphometrics, they fail to fully capture the

inherent nonlinearity in biological shape variation [8]. Many exciting ideas to account for this nonlinearity have been presented ranging from the large deformation framework [19] based on diffeomorphisms of the ambient space to modeling the variability of surfaces employing concepts from shell theory [25, 4, 14]. However, due to the inherent complexity of the involved nonlinear estimation problems the practical applicability especially in time-critical applications is limited. To address this challenge, one line of work encodes shapes using differential coordinates that provide a local description of the geometry rather than absolute positions [13, 10, 12, 24, 3]. In particular, statistical shape models based on differential coordinates have recently been successfully employed for classification of radiographic OA significantly outperforming the linear PDM [24, 3]. Typically differential coordinates are derived from the (deformation) gradient of the map that encodes the shape relative to a reference and, hence, naturally belong to the group of orientation preserving linear transformations $GL^+(3)$. However, to the best of our knowledge, previous work does not account for the rich geometric structure inherent to $GL^+(3)$. On the one hand, approaches like [27] based on the Riemannian framework are not stable according to group operations (composition and inversion) due to the lack of bi-invariant metrics for $GL^+(3)$. Anyhow, consistency with group operations is desirable as it provides invariance w.r.t. changes of reference and data coordinate systems and, thus, prevents bias due to arbitrary choices thereof. On the other hand, equipping $GL^+(3)$ with an alternative group structure as done for the *differential coordinates model* (DCM) in [24] provides bi-invariance but ignores its original, canonical structure. Furthermore, while Woods [26] proposes a similar approach for image deformation, he employs a surface representation that is not group-valued.

In this work, we derive a novel statistical shape model based on linear differential coordinates that is as-invariant-as-possible and, hence, promises increased consistency and reduced bias. To this end, we adapt the notion of bi-invariant mean as proposed in [21] employing an affine connection structure on $GL^+(3)$. Furthermore, we perform second-order statistics based on a family of Riemannian metrics providing the most possible invariance, viz. $GL^+(3)$ -left-invariance and $O(3)$ -right-invariance. We evaluate the performance of the derived model in terms of shape-based classification of pathological malformations of the human knee demonstrating superior accuracy over state-of-the-art [24, 3] approaches.

2 Differential Coordinates

In this section, we provide a concise introduction to linear differential coordinates and refer the reader to [24] for further details. We consider shapes to be instances of a class of anatomical objects that are topologically consistent, s.t. they can be represented as a left-acting deformation ϕ of a common reference \tilde{S} . We further, assume that \tilde{S} is discretized as a simplicial surface mesh with k vertices and m triangles. In order to perform analysis on local geometric details rather than absolute coordinates of a shape $S = \phi(\tilde{S})$, we can employ a differential representation given by the deformation gradient $\nabla\phi$, i.e. the 3×3

matrix of partial derivatives of ϕ . Let ϕ be orientation-preserving and affine on each triangle $\bar{T}_i \in \bar{S}$, then the derivatives are constant on each triangle with $\nabla\phi|_{\bar{T}_i} \equiv D_i \in \text{GL}^+(3)$. Note, that the deformation of a triangle fully specifies an affine map of \mathbb{R}^3 if we assume that triangle normals are mapped onto each other (cf. Kirchhoff–Love kinematic assumptions). Accordingly, a representation of a shape S in linear differential coordinates is given by $\xi = (D_1, \dots, D_m)^T$.

A key feature of this representation is that the inverse problem of mapping differential coordinates back to a deformation ϕ leads to the well-known Poisson equation

$$\Delta\phi = \nabla \cdot \xi, \quad (1)$$

where $\Delta \in \mathbb{R}^{k \times k}$ and $\nabla \cdot \in \mathbb{R}^{k \times 3m}$ denote the discrete Laplacian and divergence operator, respectively. Note, as (1) is a linear differential equation it can be solved very efficiently. Furthermore, the solutions are unique up to translations of each connected component of \bar{S} .

3 Geometric Statistics in $\text{GL}^+(3)$

In order to derive information of our geometric data we perform element-wise geometric statistics on it. Let $\{\xi^j = (D_1^j, \dots, D_m^j)^T\}_{j=1}^n$ be the set of all input shapes represented in differential coordinates. The essential components to set up a statistical shape model are a mean value and a tangent Principal Component Analysis (tPCA) [9] to analyze the input as deviations thereof.

3.1 Bi-invariant Mean

Since $\text{GL}^+(3)$ does not admit a bi-invariant metric there can not exist a bi-invariant *Riemannian* mean. Nevertheless, due to the Lie group structure there exists a naturally bi-invariant candidate for the mean in terms of the group exponential barycenter called *bi-invariant mean*. We follow hereby the work of Pennec and Arsigny [21] who delivered a comprehensive characterization and analysis on this topic. The bi-invariant mean M_i is defined through:

$$\sum_{j=1}^n \log \left(D_i^j \cdot M_i^{-1} \right) = 0, \quad (2)$$

where \log denotes the group logarithm. To solve for the unknown M_i we apply an iterative fixed point scheme:

$$M_i^{k+1} = \exp \left(\sum_{j=1}^n \log \left(D_i^j \cdot (M_i^k)^{-1} \right) \right) \cdot M_i^k, \quad (3)$$

where \exp denotes the group exponential.

The local existence and uniqueness of the bi-invariant mean have been proven for data with small enough dispersion, i.e. if the data lies within a sufficiently small normal convex neighborhood of some point of the Lie group. Furthermore, the algorithm given by Eq. (3) always converges to M_i at least with linear speed provided that the initialization is chosen sufficiently close to the data.

From Eq. (3) we see that the group logarithm and exponential of $\text{GL}^+(3)$ are essential operations required to determine the mean shape as well as for the statistical analysis in its tangent space (Sec. 3.2). However, it should be emphasized that there does not exist a *real* logarithm for every element in $\text{GL}^+(3)$. We can classify such elements by investigating the underlying eigenvalue structure. Let D be an arbitrary element in $\text{GL}^+(3)$. It is known that there always exists a *real* Jordan-Decomposition [11] $D = V \cdot E \cdot V^{-1}$ s.t. E belongs (modulo permutation) to one of the following three types:

$$\begin{aligned} \text{A: } & \begin{pmatrix} \lambda_1 & 0 & 0 \\ 0 & \lambda_2 & 0 \\ 0 & 0 & \lambda_3 \end{pmatrix}, \quad \text{where } \lambda_i \in \mathbb{R}^+, \\ \text{B: } & \begin{pmatrix} -\lambda_1 & 0 & 0 \\ 0 & -\lambda_2 & 0 \\ 0 & 0 & \lambda_3 \end{pmatrix}, \quad \text{where } \lambda_i \in \mathbb{R}^+, \lambda_1 \neq \lambda_2, \\ \text{C: } & \begin{pmatrix} \lambda_1 & \mu & 0 \\ -\mu & \lambda_1 & 0 \\ 0 & 0 & \lambda_2 \end{pmatrix}, \quad \text{where } \lambda_1 + i\mu \in \mathbb{C} \setminus \{0\}, \lambda_2 \in \mathbb{R}^+. \end{aligned}$$

As the logarithm is compatible with a change of basis it is enough to consider only matrices of the above form. Both cases A and C admit a real logarithm, contrasting case B that does not allow for its existence. This raises the question what deformation gradients could feature such an eigenvalue configuration and whether it is likely to appear. If we take a closer look at case B we see that it encodes an anisotropic scale with two negative weights. Since the respective deformation is orientation preserving it must invert two edges of a triangle and change their lengths in a non-uniform fashion. This seems to be a rather unlikely deformation, if we consider data to be aligned and without artifacts such as local overfolds. In particular, the two real word datasets we performed our experiments on (Sec. 4) did not admit any element in any input shape that came across with a deformation gradient of this structure. Neither during calculation of the mean nor during analysis.

However, in order to do statistics in $\text{GL}^+(3)$ that are robust to such extreme cases we require an alternative strategy. To this end, we propose to perform a *pseudo* logarithm operation. Let D be an element of $\text{GL}^+(3)$ with no logarithm. We define its pseudo logarithm *plog* employing polar decomposition as follows:

$$\text{plog}(D) = \text{plog}(RU) := \log(R) + \log(U)$$

In case a real $\log(D)$ exists this formula can be seen as first order (commutator free) approximation in terms of the Baker–Campbell–Hausdorff formula and for

commutating R, U this formula would be even exact. This can additionally be interpreted as a fallback to the product structure of the DCM [24]. Contrary to the logarithm, the matrix exponential always exists and can efficiently be calculated using the scaling-and-squaring method together with Padé approximations [15].

3.2 Tangent Principal Component Analysis

In the previous section we were able to circumvent the absence of a bi-invariant metric but this is no longer possible if we want to perform higher-order analysis using tPCA. While there is no bi- $\text{GL}^+(3)$ -invariant metric, we are interested in metrics that yield at least invariance under orthogonal transformations, i.e. metrics that are invariant with respect to a change of coordinates obtained by rotating or mirroring the data. Indeed, there exists exactly one family of metrics that is $\text{GL}^+(3)$ -left-invariant and $\text{O}(3)$ -right-invariant and uniquely determined up to three positive real constants [18]. We define the metric as usual via the inner product on the respective Lie algebra.

Let $X, Y \in \mathfrak{gl}(3) = \mathbb{R}^{3 \times 3}$ and $\mu, \nu, \kappa \in \mathbb{R}^+$:

$$\langle X, Y \rangle_{\mu, \nu, \kappa} := \mu \langle \text{dev sym } X, \text{dev sym } Y \rangle + \nu \langle \text{skew } X, \text{skew } Y \rangle + \frac{\kappa}{3} \text{tr}(X) \text{tr}(Y),$$

where we have used the following notation:

$$\begin{aligned} \langle \cdot, \cdot \rangle &= \langle \cdot, \cdot \rangle_2 = \text{tr}(X^T Y) && \text{(standard inner product),} \\ \text{sym } X &= \frac{1}{2}(X + X^T) && \text{(symmetric part of } X), \\ \text{skew } X &= \frac{1}{2}(X - X^T) && \text{(skew-symmetric part of } X), \\ \text{dev } X &= X - \frac{\text{tr } X}{3} I_3 && \text{(deviator of } X). \end{aligned}$$

If we consider X as *infinitesimal transformation* the above terms admit certain geometric interpretations: skew X represents the rotational part and sym X the distortion part. While the trace tr quantifies volume changes, the deviator dev represents the trace-free part and, hence, $\text{dev sym } X$ describes the shearing (volume-preserving distortion) part of X . Furthermore, the above inner product features two interesting properties:

$$\begin{aligned} \langle X, Y \rangle_{1,1,1} &= \langle X, Y \rangle && \text{for all } X, Y \in \mathfrak{gl}(3), \\ \langle X, Y \rangle_{\mu, \nu, \kappa} &= 0 && X \in \mathfrak{so}(3), Y \text{ symmetric.} \end{aligned}$$

Hence, this family of metrics can be seen as natural generalization of the standard metric arising from the standard inner product for matrices. Let us assume to have n input shapes with m triangles each, then we perform tPCA in the tangent space $T_M(\text{GL}^+(3))^m$ at the differential coordinates of the mean shape

$M = (M^1, \dots, M^m)$. The $(p+1)$ -th mode of variation is hereby given as:

$$v_{p+1} = \arg \max_{g_{\mu, \nu, \kappa}^M(v, v)=1} \sum_{i=1}^n \sum_{l=1}^p g_{\mu, \nu, \kappa}^M(v_l, \log(D_i))^2 + g_{\mu, \nu, \kappa}^M(v, \log(D_i))^2, \quad (4)$$

where $D_i = (D_i^1, \dots, D_i^m)$, \log is applied component-wise and $g_{\mu, \nu, \kappa}^M = \sum g_{\mu, \nu, \kappa}^{M^j}$ is the metric emerging from $\langle \cdot, \cdot \rangle_{\mu, \nu, \kappa}$.

4 Experiments and Results

The following experiments are performed utilizing (rounded) metric parameters $\mu = 0.1$, $\nu = 29.42$, $\kappa = 1.3$ that have been found conducting *hyper parameter optimization* (HPO) w.r.t. best performance in our classification experiment. HPO was carried out within the Scikit-Optimize¹ python framework performing a sequential optimization using decision trees (forest_minimize) on the cubical domain $[0.05, 1000]^3$.

Data We employ two datasets:

(i) Distal femora (see Fig. 2) from the Osteoarthritis Initiative (OAI) for 58 severely diseased and 58 healthy subjects that were also used for evaluation in [24, 3] and are publicly available as segmentations² [2]. For a detailed list of the exact subjects that are included in the experiment as well as their disease state we refer to the supplemental material of [3]. We used the surface meshes as provided by the authors (in particular the correspondences) and we refer to [24] for further details on the creation of the dataset.

(ii) Skeletal human hand (see Fig. 3) taken from the publicly available data³ of [16] that is based on data of the Large Geometric Models Archive from the Georgia Institute of Technology.

Knee Osteoarthritis Classification OA is i.a. characterized by changes of the shape of bones composing the knee. With this experiment we want to investigate the proposed $GL^+(3)$ model's sensitivity w.r.t. pathological shape changes and thus its ability to classify knee OA for the OAI dataset of distal femora. To achieve this, we utilize a simple support vector machine (SVM) with linear kernel directly on the 115-dimensional space of shape weights. These weights are the vectors of coefficients w.r.t. the principal modes for each shape. The weights serve as input features to the SVM. The classifier is trained on a balanced set (healthy/diseased) of feature vectors for different shares of randomly chosen data varying from 10% to 90% whereas the testing is performed on the respective complement. Since we have some randomness in our experimental design we carry out the experiment 10000 times for each partition and consider the mean accuracy and the standard deviation. We compare our method to the PDM [7] as well as to the in a way related DCM [24] and the recent *fundamental*

¹ <https://scikit-optimize.github.io>

² <https://doi.org/10.12752/4.ATEZ.1.0>

³ http://graphics.stanford.edu/~niloy/research/shape_space/shape_space_sig.07.html

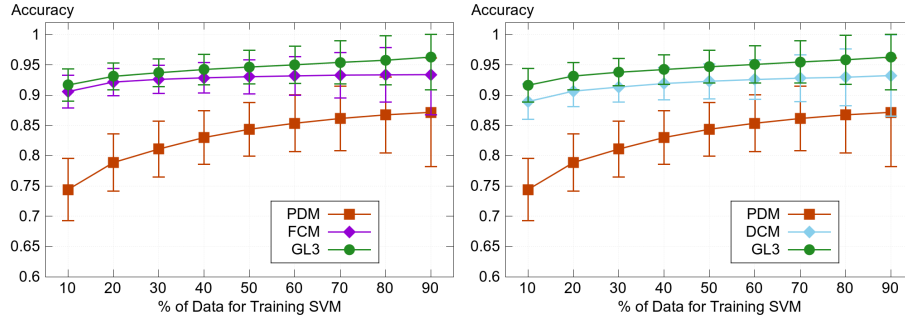


Fig. 1. OA classification experiment for the proposed $GL^+(3)$ model, PDM [7] and the recent FCM [3] (left) and the related DCM [24] (right). The accuracy of the $GL^+(3)$ model ranges from 91.6% (at 10% training) to 96.3% (at 90% training).

coordinate model (FCM) [3], which both achieved highly accurate classification results. To this end, we employ the above outlined classifier setup using the respective model specific shape weights.

Figure 1 shows the results in terms of average accuracy and standard deviation. The accuracy of the $GL^+(3)$ model ranges from 91.6% (at 10% training) to 96.3% (at 90% training). Note that solely the proposed $GL^+(3)$ method achieves an accuracy of over 91% in case of sparse (10%) training data.

Qualitative Evaluation We perform two qualitative experiments.

(i) A comparison of the mean shape of the OAI dataset as determined by the DCM as well as the proposed $GL^+(3)$ model. To achieve this we align both shapes and calculate the surface distance between them. Both mean shapes are highly similar as can be seen in Fig. 2.

(ii) An analysis of the skeletal hand dataset. We calculate the mean shape of the two input poses, perform tPCA and (visually) investigate the resulting trajectory connecting the two input shapes through the mean w.r.t. plausibility. As shown in Fig. 3 the principal mode shows natural nonlinear deformation characteristics.

5 Conclusion and Future Work

In this work, we presented a novel nonlinear statistical shape model based on $GL^+(3)$. The model utilized the bi-invariant Lie group mean and a tangent principal component analysis employing a $GL^+(3)$ -left-invariant, $O(3)$ -right-invariant metric in $GL^+(3)$. It can thus be considered as as-invariant-as-possible w.r.t. the canonical $GL^+(3)$ structure of the deformation gradient. We have shown that the proposed model possess a high descriptiveness w.r.t. natural biological differences in shape. In order to determine the parameters of the metric we applied a hyper parameter optimization targeting classification accuracy. In particular, we conducted experiments on OA classification achieving results that are superior to those of the state-of-the-art models [24, 3].

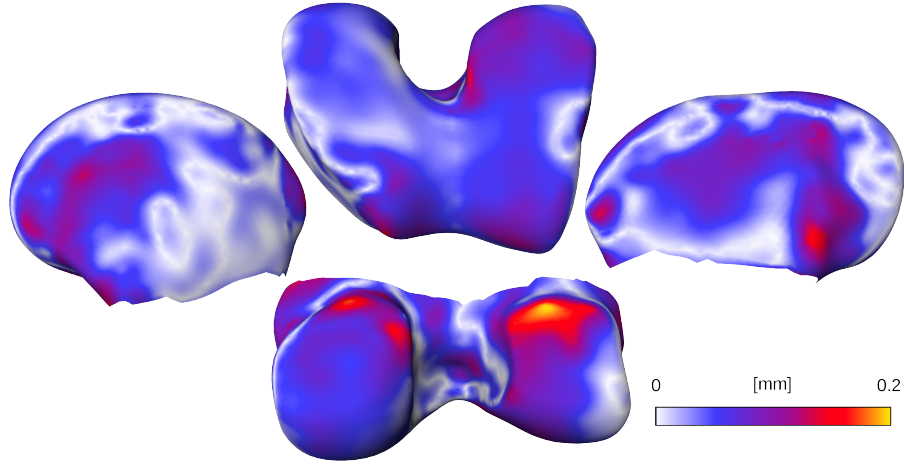


Fig. 2. Deviations of mean distal femur shape as calculated with the proposed $GL^+(3)$ model and the DCM [24]. Absolute values of the surface distance are plotted color-coded on the DCM mean shape.

We consider it valuable and interesting to also investigate the purely Riemannian perspective associated with the above metric and compare it to our present work. Although geodesics can be evaluated in closed form for a given direction and the existence of a shortest geodesic connecting two arbitrary points is theoretically guaranteed, no closed form solution to determine the direction of one (and not necessarily the shortest) connecting geodesic is known [18].

Acknowledgments

The authors are funded by the Deutsche Forschungsgemeinschaft (DFG, German Research Foundation) under Germany’s Excellence Strategy – The Berlin Mathematics Research Center MATH+ (EXC-2046/1, project ID: 390685689). Furthermore, we are grateful for the open-access OAI dataset of the Osteoarthritis Initiative, that is a public-private partnership comprised of five contracts (N01-AR-2-2258; N01-AR-2-2259; N01-AR-2-2260; N01-AR-2-2261; N01-AR-2-2262) funded by the National Institutes of Health, a branch of the Department of Health and Human Services, and conducted by the OAI Study Investigators. Private funding partners include Merck Research Laboratories; Novartis Pharmaceuticals Corporation, GlaxoSmithKline; and Pfizer, Inc. Private sector funding for the OAI is managed by the Foundation for the National Institutes of Health. This manuscript was prepared using an OAI public use data set and does not necessarily reflect the opinions or views of the OAI investigators, the NIH, or the private funding partners.

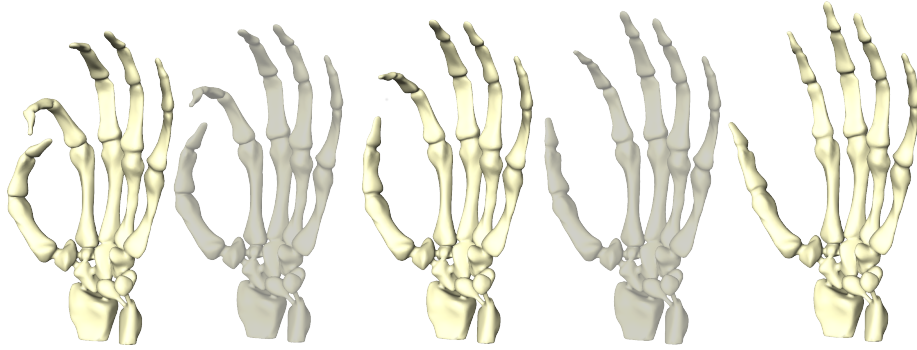


Fig. 3. Trajectory as calculated with the proposed $GL^+(3)$ model connecting the input shapes (left, right) via the exponential mean (center) showing natural deformation characteristics.

References

1. Ambellan, F., Lamecker, H., von Tycowicz, C., Zachow, S.: Statistical shape models - understanding and mastering variation in anatomy. In: Rea, P.M. (ed.) *Biomedical Visualisation*, vol. 3, pp. 67 – 84. Springer, 1 edn. (2019)
2. Ambellan, F., Tack, A., Ehlke, M., Zachow, S.: Automated segmentation of knee bone and cartilage combining statistical shape knowledge and convolutional neural networks. *Med Image Anal* **52**, 109–118 (2019)
3. Ambellan, F., Zachow, S., von Tycowicz, C.: A surface-theoretic approach for statistical shape modeling. In: *Proc. Medical Image Computing and Computer Assisted Intervention (MICCAI)* (2019), accepted for publication
4. Brandt, C., von Tycowicz, C., Hildebrandt, K.: Geometric flows of curves in shape space for processing motion of deformable objects. *Comput Graph Forum* **35**(2) (2016)
5. Bredbenner, T.L., Eliason, T.D., Potter, R.S., Mason, R.L., Havill, L.M., Nicoletta, D.P.: Statistical shape modeling describes variation in tibia and femur surface geometry between control and incidence groups from the osteoarthritis initiative database. *J Biomech* **43**(9), 1780–1786 (2010)
6. Conaghan, P.G., Kloppenburg, M., Schett, G., Bijlsma, J.W., et al.: Osteoarthritis research priorities: a report from a eular ad hoc expert committee. *Annals of the rheumatic diseases* **73**(8), 1442–1445 (2014)
7. Cootes, T.F., Taylor, C.J., Cooper, D.H., Graham, J.: Active shape models-their training and application. *Comput Vis Image Underst* **61**(1), 38–59 (1995)
8. Davis, B.C., Fletcher, P.T., Bullitt, E., Joshi, S.: Population shape regression from random design data. *Int J Comput Vis* **90**(2), 255–266 (2010)
9. Fletcher, P., Lu, C., Pizer, S., Joshi, S.: Principal geodesic analysis for the study of nonlinear statistics of shape. *IEEE Trans Med Imaging* **23**(8), 995–1005 (2004)
10. Freifeld, O., Black, M.J.: Lie bodies: A manifold representation of 3d human shape. In: *ECCV*. pp. 1–14. Springer (2012)
11. Gallier, J.: Logarithms and square roots of real matrices existence, uniqueness and applications in medical imaging. *arXiv preprint arXiv:0805.0245* (2018)

12. Gao, L., Lai, Y.K., Liang, D., Chen, S.Y., Xia, S.: Efficient and flexible deformation representation for data-driven surface modeling. *ACM Trans Graph* **35**(5), 158 (2016)
13. Hasler, N., Stoll, C., Sunkel, M., Rosenhahn, B., Seidel, H.P.: A statistical model of human pose and body shape. *Comput Graph Forum* **28**(2), 337–346 (2009)
14. Heeren, B., Zhang, C., Rumpf, M., Smith, W.: Principal geodesic analysis in the space of discrete shells. *Comput Graph Forum* **37**(5), 173–184 (2018)
15. Higham, N.J.: The scaling and squaring method for the matrix exponential revisited. *SIAM Journal on Matrix Analysis and Applications* **26**(4), 1179–1193 (2005)
16. Kilian, M., Mitra, N.J., Pottmann, H.: Geometric modeling in shape space. *ACM Transactions on Graphics (SIGGRAPH)* **26**(3), #64, 1–8 (2007)
17. Lawrence, R.C., Felson, D.T., Helmick, C.G., Arnold, L.M., Choi, H., Deyo, R.A., Gabriel, S., Hirsch, R., Hochberg, M.C., Hunder, G.G., et al.: Estimates of the prevalence of arthritis and other rheumatic conditions in the united states: Part ii. *Arthritis & Rheumatology* **58**(1), 26–35 (2008)
18. Martin, R.J., Neff, P.: Minimal geodesics on $GL(n)$ for left-invariant, right- $O(n)$ -invariant Riemannian metrics. *Journal of Geometric Mechanics* **8**(3), 323–357 (2016)
19. Miller, M.I., Trouné, A., Younes, L.: Hamiltonian systems and optimal control in computational anatomy: 100 years since d’arcy thompson. *Annual review of biomedical engineering* **17**, 447–509 (2015)
20. Neogi, T., Bowes, M.A., Niu, J., Souza, K.M., Vincent, G.R., Goggins, J., Zhang, Y., Felson, D.T.: Magnetic resonance imaging-based three-dimensional bone shape of the knee predicts onset of knee osteoarthritis. *Arthritis Rheum* **65**(8), 2048–2058 (2013)
21. Pennec, X., Arsigny, V.: Exponential barycenters of the canonical Cartan connection and invariant means on Lie groups. In: *Matrix Information Geometry*, pp. 123–166. Springer (2013)
22. Thomson, J., O’Neill, T., Felson, D., Cootes, T.: Automated shape and texture analysis for detection of osteoarthritis from radiographs of the knee. In: *MICCAI*, pp. 127–134. Springer (2015)
23. Thomson, J., O’Neill, T., Felson, D., Cootes, T.: Detecting Osteophytes in Radiographs of the Knee to Diagnose Osteoarthritis, pp. 45–52. Springer International Publishing (2016)
24. von Tycowicz, C., Ambellan, F., Mukhopadhyay, A., Zachow, S.: An efficient Riemannian statistical shape model using differential coordinates. *Med Image Anal* **43**, 1–9 (2018)
25. von Tycowicz, C., Schulz, C., Seidel, H.P., Hildebrandt, K.: Real-time nonlinear shape interpolation. *ACM Trans Graph* **34**(3), 34:1–34:10 (2015)
26. Woods, R.P.: Characterizing volume and surface deformations in an atlas framework: theory, applications, and implementation. *NeuroImage* **18**(3), 769–788 (2003)
27. Zacur, E., Bossa, M., Olmos, S.: Multivariate tensor-based morphometry with a right-invariant riemannian distance on $gl+(n)$. *Journal of mathematical imaging and vision* **50**(1-2), 18–31 (2014)